A New Reconfigurable Antenna Scheme and its Application to Vehicle-to-Vehicle Communications

Petros S. Bithas, Antonis Aspreas, and Athanasios G. Kanatas
Department of Digital Systems, University of Piraeus, Greece, e-mail: {pbithas;aspreas;kanatas}@unipi.gr

***Abstract*—Reconfigurable antenna arrays provide important advantages such as reduction on the number of the physical antennas or reduced hardware complexity in terms of receiving radio frequency chains. Both these properties are critical in vehicle-to-vehicle (V2V) communication systems, which are characterized by inflexible dimensions and cost constraints. In this paper, a new pattern reconfigurable antenna array selection scheme is proposed that aims to reduce the complexity of the traditional antenna selection techniques. For this scheme, an analytical statistical framework is developed for characterizing the output signal-to-noise ratio (SNR). The analysis is general enough to take into consideration the impact of correlation on the antenna patterns. Special cases are also studied assuming independence between the patterns, while the diversity and coding gains are also evaluated. The performance is analysed using the criteria of outage probability and the average bit error probability. Moreover, the new scheme is applied in a V2V communication scenario based on the IEEE 802.11p standard, while it is compared with other well-known receivers under different channel model conditions.**

***Index Terms*- Diversity gain, non-stationary channel conditions, reconfigurable antenna arrays, reduced complexity, vehicle-to-vehicle communications.**

I. Introduction

Diversity systems have been widely adopted in various wireless communication scenarios for improving the spectral and power efficiency. The basic principle of this powerful technique is that the different signal paths have low probability of simultaneously be affected by deep fades. Various methods for achieving diversity exist including: space, angle, polarization, frequency, multipath, and time. Under the same principle, pattern reconfigurable antenna arrays have been proposed for further improving the performance of wireless communication systems. In particular, numerous works have considered "antenna selection" based on different radiation pattern, e.g., [1]–[5]. The main idea in these schemes is that the total number of antennas is divided into different groups, which are created by a single physical antenna supporting multiple radiation patterns or states. Such an approach, results in clear benefits such as fewer physical antennas as well as fixed hardware complexity in terms of receiving radio frequency (RF) chains [6]. Moreover, a common assumption in most of the previous works is that independent channel conditions were exploited. Nevertheless, despite the obvious advantages of these systems, the open technical literature related with the application of reconfigurable systems to intervehicular communications scenarios is relatively sparse, e.g., [7].

In general, vehicular ad-hoc networks (VANET)s represent an integral part of the intelligent transportation systems (ITS)s that has gained an important interest by the scientific community over the past several years. These systems enable the vehicle-to-vehicle (V2V) communications and can be applied in a variety of communication scenarios ranging from road-safety and energy-saving improvements to comfort and infotainment. However, in contrast to the traditional cellular-mobile radio link, the V2V propagation channel is much more dynamic, since it consists of two non-stationary transceivers, closely located to the ground level. In this context, many works have investigated the performance improvement of V2V communication systems based on diversity reception techniques, e.g., [8]–[10]. For example, in [9], the performance of various diversity schemes has been analyzed in single and double scattering channels. However, despite the notable contribution of these works, they are mainly based on antenna switching approach. As a result, non-negligible performance losses are expected due to the continuous switching operations, while an increase on the cost of the antennas is expected due to the number of well-matched and response-stable microwave switches [11].

In this paper, we propose a novel reconfigurable antenna scheme that is based on a new state selection approach. The new scheme employs two RF chains that support reconfigurable antenna arrays with two states each. This approach allows us to achieve an important diversity gain, satisfying also the strict constraints that exist in the vehicle dimensions as well as cost. In order to further reduce the complexity of the proposed scheme, in each reception period, the antenna reconfigurability is performed in only one of the two RF chains. For this new approach, a novel analytical framework is developed for evaluating its statistical characteristics. The new framework is general enough to take into account the correlation between the antenna patterns that is present in real-world situations. Moreover, as an application example this scheme has been employed in a V2V communication scenario that is based on IEEE 802.11p standard and its performance is analyzed under different channel conditions.

The rest of the paper is organized as follows. Section II includes the system and channel model under investigation, where the mode of operation of the proposed scheme is also described. In Section III, the analytical framework of important statistical characteristics of the proposed approach is provided. In Section IV, numerical results are given for important performance measures such as the outage probability (OP) and the average bit error probability (BEP). Moreover, in the same section, simulation results based on IEEE 802.11p standard and the proposed scheme are also provided. Finally, Section V concludes this paper.

II. System and Channel Model

We consider a communication system with one transmitter (with one RF chain) and one receiver with two RF chains. In each receiving antenna, reconfigurable antenna arrays exist with two modes (or states) of operation based on the radiation pattern characteristics, i.e., shape, direction, polarization. In the proposed scheme, during a given period of reception, the system is continuously using a specific radiation pattern from one of the two receivers' RF chain, while from the other one, it selects the state that provides the best performance in terms of the received signal-to-noise ratio (SNR). Such an approach, where one of the two RF chains is always based on a specific pattern, without any kind of examinations, provides clear practical benefits in terms of synchronization, channel estimation, while also offers reduced number of switching operations. It should be noted that switching among branches (or states) not only consumes power, but also reduces the data throughput in a transmit diversity configuration and leads to inaccurate phase estimates [11]. The reduced amount of switches that the proposed scheme offers, further decreases in cases where time correlated wireless medium exists. In particular, under time correlated fading conditions, assuming that a tagged antenna pattern is selected in time instance t, based on the maximum SNR criterion, it is very likely that in the next instance, $t+\tau$, the same pattern selection will be also made. However, in our theoretical analysis, in order to provide convenient closed-form expression time-correlated conditions have been omitted.

Assuming that γ_i, with $i \in \{1,2,3,4\}$, denotes the instantaneous received SNR based on the ith state, the mode of operation of the proposed scheme is depicted in Fig. 1. In this figure, we have assumed that $\gamma_{\max} = \max\{\gamma_j, \gamma_{j+1}\}$, with $j \equiv 3$ if $i \in \{1,2\}$, else $j \equiv 1$. Thus, assuming independence between γ_i and $\gamma_{\max}$, it is not difficult to recognize that the total instantaneous output SNR is given by

$$\gamma_{\text{out}} \triangleq \gamma_i + \gamma_{\max}. \tag{1}$$

In that case, the moment generating function (MGF) of the output SNR for the new scheme is given by

$$\mathcal{M}_{\gamma_{\text{out}}} = \mathcal{M}_{\gamma_i}(s)\mathcal{M}_{\gamma_{\max}}(s). \tag{2}$$

The previous expression apply to any fading scenario. Here, we will focus on the Rayleigh multipath fading model, which typically agrees very well with experimental data for mobile systems where no line-of-sight path exists between the transmitter's and receiver's antennas. Assuming identically distributed fading conditions, the instantaneous received SNR of the ith state follows the exponential distribution with probability density function (PDF) given by

$$f_{\gamma_i}(\gamma) = \frac{1}{\overline{\gamma}} \exp\left(-\frac{\gamma}{\overline{\gamma}}\right) \tag{3}$$

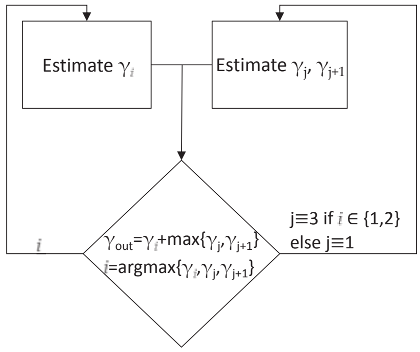

Fig. 1. Mode of operation of the proposed scheme.

where $\overline{\gamma}$ denotes the average received SNR. The corresponding expressions for the cumulative distribution function (CDF) and the MGF are given as

$$F_{\gamma_i}(\gamma) = 1 - \exp\left(-\frac{\gamma}{\overline{\gamma}}\right) \tag{4a}$$

$$\mathcal{M}_{\gamma_i}(s) = \frac{1}{1+s\overline{\gamma}}. \tag{4b}$$

In the following section, we will provide analytical expressions for important statistical metrics of the output SNR for the system under consideration.

III. Statistical Characteristics

A. Generic Scenario

Here, we consider the practical important scenario where correlation exists between the antenna patterns that are provided by the reconfigurable antenna array and are available to the RF chain. Correlation between the antenna patterns is a reasonable assumption since in many cases due to the proximity of the antennas as well as the surrounding environment it is very likely that the antenna radiation patterns will be correlated. As a consequence, the instantaneous received SNRs γ_j and γ_{j+1}, based on $j, j+1$ patterns, will be also correlated[1], with bivariate PDF given by

$$\begin{aligned} f_{\gamma_j,\gamma_{j+1}}(x_1,x_2) = &\frac{1}{\overline{\gamma}^2(1-\rho)} \exp\left[-\frac{x_1+x_2}{(1-\rho)\,\overline{\gamma}}\right] \\ &\times I_0\left(\frac{2\sqrt{\rho x_1 x_2}}{(1-\rho)\overline{\gamma}}\right) \end{aligned} \tag{5}$$

where ρ denotes the correlation coefficient between γ_j and γ_{j+1} and $I_v(\cdot)$ denotes the first kind modified Bessel function of the vth order [12, eq. (8.845)].

Theorem 1: Let $\gamma_i, \gamma_j, \gamma_{j+1}$ denote three random variables (RV)s following exponential distribution with marginal PDF given by (3). Moreover, let γ_{out} defined as in (1), with γ_i being independent from both γ_j and γ_{j+1}, while γ_j, γ_{j+1} are

[1] In this work, it is assumed that the reconfigurable antennas between the two RF chains are separated by a distance large enough that guarantees fully decorrelation and thus correlation exists only between states j and $j+1$.

correlated RVs with joint PDF given by (5). The PDF of $\gamma_{\rm out}$ is given by

$$f_{\gamma_{\rm out}}(\gamma)=\frac{2}{\overline{\gamma}^2}\exp\left(-\frac{\gamma}{\overline{\gamma}}\right)\times\left\{\gamma+Q_1\left[\sqrt{\frac{2\rho\gamma}{\overline{\gamma}(1-\rho)}},\sqrt{\frac{2\gamma}{\overline{\gamma}(1-\rho)}}\right]\left(\frac{2\overline{\gamma}}{1-\rho}-\gamma\right)+\frac{g(\gamma,0)}{1-\rho}(\gamma-\overline{\gamma})-\frac{\overline{\gamma}}{1-\rho}+\frac{\sqrt{\rho}\gamma}{1-\rho}g(\gamma,1)\right\} \quad (6)$$

where

$$g(x,i)=\exp\left(-\frac{1+\rho}{\overline{\gamma}(1-\rho)}x\right)I_i\left(\frac{2\sqrt{\rho}x}{\overline{\gamma}(1-\rho)}\right),$$

and $Q_1(\cdot,\cdot)$ denoting the first order Marcum Q-function [13, eq. (4.33)].

Proof: See the Appendix. ■

Corollary 1: The CDF of $\gamma_{\rm out}$ is given by

$$F_{\gamma_{\rm out}}(\gamma)=2\left\{F_{\gamma_i}(\gamma)-\left[\frac{1}{2}\left(1+\exp\left(-\frac{\kappa\gamma}{2}\right)\times I_0\left(\frac{2\sqrt{\rho}\gamma}{\overline{\gamma}(1-\rho)}\right)\right)-\exp\left(-\frac{\gamma}{\overline{\gamma}}\right)\times Q_1\left[\sqrt{\frac{2\rho\gamma}{\overline{\gamma}(1-\rho)}},\sqrt{\frac{2\gamma}{\overline{\gamma}(1-\rho)}}\right]\right]\right\}-\overline{\gamma}f_{\gamma_{\rm out}}(\gamma) \quad (7)$$

where

$$\kappa=\frac{2}{\overline{\gamma}}+\frac{2(1+\rho)}{\overline{\gamma}(1-\rho)}.$$

Proof: Since $F_{\gamma_i}(\gamma)=\mathcal{L}^{-1}\left\{\mathcal{M}_{\gamma_i}(s)/s,\gamma\right\}$, substituting (3a) and (A-3) in (A-2), following a similar approach as the one described in the Appendix and employing [14, eq. (55)], results to (7). ■

B. Independent Channel States

Assuming independence between γ_j and γ_{j+1}, the PDF of $\gamma_{\rm max}$ is given by

$$f_{\gamma_{\rm max}}(\gamma)=\sum_{i=1}^{2}\binom{2}{i}(-1)^{i+1}\frac{i}{\overline{\gamma}}\exp\left(-\frac{i\gamma}{\overline{\gamma}}\right). \quad (8)$$

Based on it, the corresponding MGF expression can be derived as

$$\mathcal{M}_{\gamma_{\rm max}}(s)=\sum_{i=1}^{2}\binom{2}{i}(-1)^{i+1}\frac{i}{i+\overline{\gamma}s}. \quad (9)$$

Substituting (3b) and (9) in (2) and applying the inverse Laplace transform, yields the following simplified expression for the PDF of $\gamma_{\rm out}$

$$f_{\gamma_{\rm out}}(\gamma)=\frac{2}{\overline{\gamma}}\exp\left(-\frac{\gamma}{\overline{\gamma}}\right)\left[\frac{\gamma}{\overline{\gamma}}+\exp\left(-\frac{\gamma}{\overline{\gamma}}\right)-1\right]. \quad (10)$$

Based on (10), the corresponding expression for the CDF of $\gamma_{\rm out}$ can directly be evaluated as

$$F_{\gamma_{\rm out}}(\gamma)=1-\exp\left(-\frac{2\gamma}{\overline{\gamma}}\right)-\frac{2\gamma}{\overline{\gamma}}\exp\left(-\frac{\gamma}{\overline{\gamma}}\right). \quad (11)$$

C. Asymptotic Analysis

The exact expression for $F_{\gamma_{\rm out}}(\gamma)$ given in (7) cannot be used to obtain a clear physical insight of the system's performance. Therefore, here, a simplified asymptotic expression for $F_{\gamma_{\rm out}}(\gamma)$ will be derived and used to study the diversity and coding gains. For the general case where correlation exists between γ_j and γ_{j+1}, assuming higher values of the average input SNR and using [14, eq. (2)], a simplified expression for the PDF of $\gamma_{\rm max}$ can be extracted as

$$f_{\gamma_{\rm max}}(\gamma)\approx\frac{2}{\overline{\gamma}}\exp\left(-\frac{\gamma}{\overline{\gamma}}\right)\left[1-\exp\left(-\frac{\gamma}{\overline{\gamma}(1-\rho)}\right)\right]. \quad (12)$$

Moreover, since for higher values of the average SNR $f_{\gamma_i}(\gamma)\approx\frac{1}{\overline{\gamma}}$, and based on (12) as well as the analysis presented in the Appendix, the following simple expression for the PDF of $\gamma_{\rm out}$ is derived

$$f_{\gamma_{\rm out}}(\gamma)\approx\frac{\gamma^2}{1-\rho}\frac{1}{\overline{\gamma}^3}. \quad (13)$$

The corresponding CDF expression is given by

$$F_{\gamma_{\rm out}}(\gamma)\approx\frac{\gamma^3}{3(1-\rho)}\frac{1}{\overline{\gamma}^3}. \quad (14)$$

D. Performance Evaluation

Using the previously derived results, important performance metrics of the scheme under consideration will be analytically studied. More specifically, the performance will be studied using the criteria of OP and the BEP.

1) Outage Probability: The OP is defined as the probability that the instantaneous received SNR falls below a predetermined threshold $\gamma_{\rm T}$. Therefore, in our case, the OP can be directly evaluated as $P_{\rm out}=F_{\gamma_{\rm out}}(\gamma_T)$. It is obvious that (14) is of the form $(G_c\overline{\gamma})^{-G_d}$, where G_d represents the diversity gain and $G_c=\left[\frac{\gamma_T^3}{3(1-\rho)}\right]^{-1/3}$ is the coding gain. Thus, from (14), it is clear that the correlation between the branches does not affect the diversity gain of the system under consideration, which is always equal to 3, but only the coding gain. Nevertheless, as the correlation between the antennas increases, the coding gain decreases and thus the OP performance of the system will also decrease.

E. Average Bit Error Probability

Using the previously derived MGF expressions for $\gamma_{\rm out}$ and following the MGF-based approach, the BEP can be readily evaluated for a variety of modulation schemes [13]. More specifically, the BEP can be calculated: *i)* directly for non-coherent differential binary phase shift keying (DBPSK), that is $P_{\rm b}^{DBPSK}=0.5\mathcal{M}_{\gamma_{\rm out}}(1)$ and *ii)* via numerical integration for Gray encoded M-PSK, that is $P_{\rm b}^{M-PSK}=\frac{1}{\pi\log_2 M}\int_0^{\pi-\pi/M}\mathcal{M}_{\gamma_{\rm out}}\left[\frac{\log_2 M\sin^2(\pi/M)}{\sin^2\phi}\right]d\phi$.

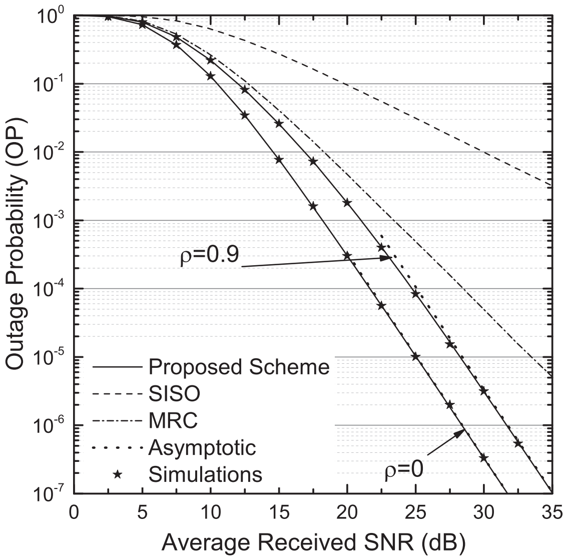

Fig. 2. OP vs the average received SNR and for different values of ρ.

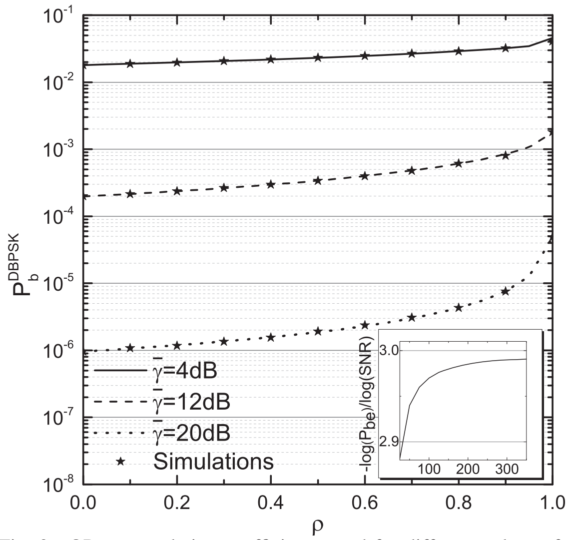

Fig. 3. OP vs correlation coefficient ρ and for different values of $\overline{\gamma}$.

IV. Numerical Results

In this section, based on the previous presented theoretical analysis, several numerically evaluated performance results are provided. These results include an OP investigation, using (7), (11), and (14), and a BEP analysis which can be evaluated with the aid of (2), (3b), (9) and (A-1). Moreover, as an application example, the proposed scheme is also employed in a V2V communication scenario using a IEEE 802.11p-based simulator.

In Fig. 2, the OP is plotted as a function of the average received SNR for different values of the correlation coefficient ρ. For comparison purposes the corresponding performances of single input single output (SISO) and maximal ratio combiner (MRC) diversity (with two RF chains) receivers have been also included. It is shown a clear diversity gain of the proposed scheme, as compared to the single receiver. Moreover,

TABLE I
Simulator Parameters.

Parameters	Value
Center Frequency	5.9GHz
Bandwidth	10MHz
Total Subcarriers	64
Effective Subcarriers	52
Guard Subcarriers	12
OFDM symbol duration	8μs
OFDM Symbols per Frame	100
Number of Frames	10^4
Coding Rate	1/2
Modulation	BPSK
Fading Model	Rayleigh

the proposed scheme also outperforms MRC even in cases where relative strong correlation exists between the branches. Moreover, the asymptotic curves, which are also included in the same figure, approximate quite well the exact ones even for moderate values of the average SNR, i.e., 20dB, while the approximation improves for lower values of ρ.

In Fig. 3, the BEP of DBPSK is plotted as a function of the correlation coefficient ρ, for different values of the average received SNR. It is shown that the performance decreases with the increase of ρ. Moreover, the performance decreases with the decrease of $\overline{\gamma}$, as expected. However, it is interesting to note that the performance deterioration due to the increase of ρ is more important for higher values of the correlation coefficient. Finally, also in the same figure, assuming $\rho = 0$, the diversity order, defined as $-\log\left(P_b^{\mathrm{DBPSK}}\right)/\log(\mathrm{SNR})$, is plotted as a function of the SNR. As it is depicted in this figure, as the SNR tends to infinity, the diversity order approaches 3, verifying the analysis provided in the previous section. Computer simulation performance results are also included in Figs. 2 and 3, verifying in all cases the validity of the proposed theoretical approach.

A. IEEE 802.11p Application Example

A physical layer simulator was developed in MATLAB for the evaluation of the proposed diversity scheme. The simulator uses a standardized transmission model based on IEEE 802.11p, which is the prime protocol for V2V communications [15]. Fig. 4 presents the block diagram of the simulator's system architecture. Next, a few details related with the simulation parameters are provided. The binary data are coded and modulated through orthogonal frequency division multiplexing (OFDM). Although the total number of subcarriers is $N = 64$, only $N_{eff} = 48$ subcarriers are used for data transmission and $N_{pilot} = 4$ subcarriers are used for pilots transmission. 10 short and 2 long preambles are added as header to the total OFDM symbols for a proper frame construction. The receiver consists of 2 RF chains with 2 states of operation at each RF chain. In addition to the proposed scheme, a SISO and a MRC

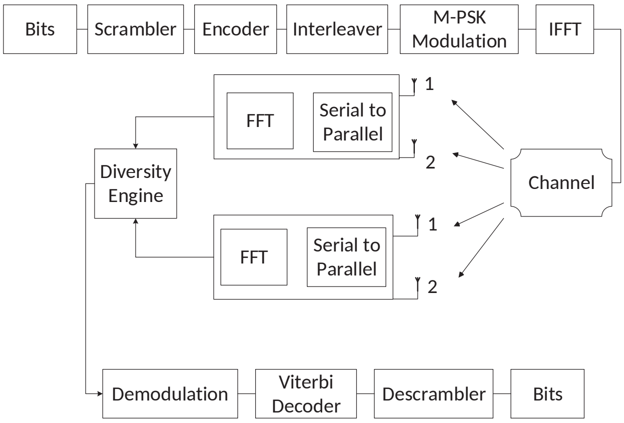

Fig. 4. Simulator block diagram.

TABLE II
DIVERSITY RECEIVERS PARAMETERS.

Receiver	RF chains	Total States	Used Antennas
MRC	2	2	2
proposed scheme	2	4	2

receiver are also implemented for comparison purposes. In the numerical analysis, the wide sense stationary uncorrelated scattering (WSSUS) assumption was assumed and flat fading Rayleigh channel was used.

In order to evaluate the performance of each diversity receiver, a BEP vs SNR diagram is derived, by means of Monte Carlo simulation. To compromise between complexity and fidelity, the noise level is normalized analogous to the desired SNR value and the transmitted signal's power is normalized to unity. In addition each scheme is simulated with perfect channel state information (CSI) knowledge at the receiver. For each SNR value 10^4 frames are transmitted. Table I summarizes the parameters used for the simulator implementation.

Fig. 5 shows the average BEP vs SNR for each diversity scheme with antennas number specified by Table II. The proposed scheme outperforms SISO, as expected. It also provides better performance from MRC, since it exploits the additional diversity gain offered by the multiple radiation patterns. It is noted that since complexity is translated to hardware processing time, the proposed scheme is a suitable receiver for fast time varying wireless medium, such as those that are typical on intervehicular communication environments, where processing time is not a negligible design parameter.

Further evaluation of the proposed scheme has been performed. Based on [16], a tap delay channel model on the 5 GHz band was developed. A major difference between the model proposed in [16] and the traditional Rayleigh one, is that the non-stationary characteristics of the channel were taken into consideration. Based on the empirical results derived from the measurement campaigns in [16], the Weibull distributed

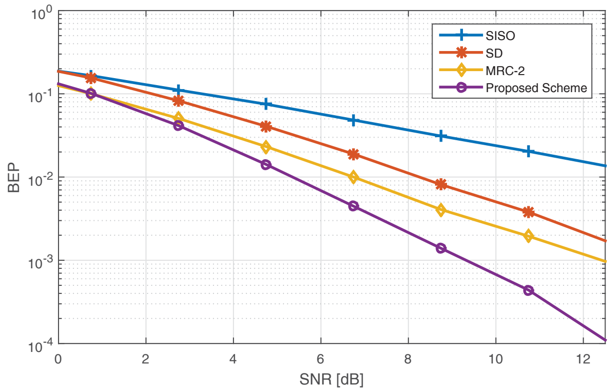

Fig. 5. Average BEP vs average SNR for the proposed scheme, MRC, SD, and SISO.

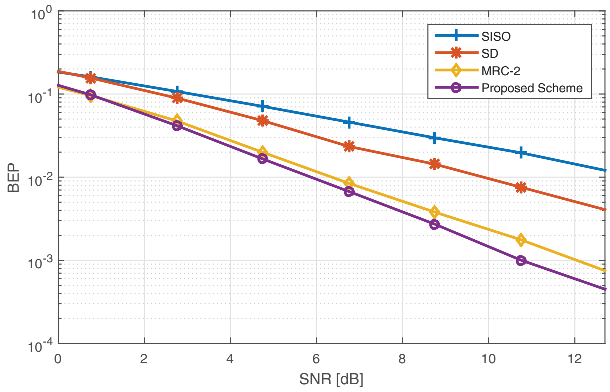

Fig. 6. Average BEP vs average SNR for the proposed scheme, MRC, SD, and SISO.

channel was proposed as a good candidate for modelling such environments. In this model, each channel tap owns Weibull statistical properties, where the shape and scale factors are defined based on the measurement results. Since for more realistic simulation results there is a need to implement time variation, time correlation was inserted between the samples of each tap. Moreover, the probability of correlation existence between two consecutive time instances obeys a simple Markov process, where transition probabilities are empirically derived. This time variation on the channel model implementation, adds the non-stationary characteristics, that are evident on V2V communication scenarios. In addition, tap amplitudes are also correlated, with correlation properties being extracted by the measurements. The measurement campaign took place on four different environments, typically characterized as "Urban with Antenna Outside the Vehicle", "Urban-Antenna Inside Car", "Open-Area High Traffic Density" and "Open-Area Low Traffic Density". From the four different environments that were implemented, the one that is characterized as "Urban with antenna outside the vehicle" was chosen for the purposes of the simulation. Moreover, no correlation was assumed between the receiving antennas. Figure 6 shows the average BEP vs SNR for each diversity scheme for a single input single output (SIMO) non stationary V2V channel. The performance degradation that is obvious, is caused by the channel's non stationarity characteristics. However, it is noted that the BEP-SNR curves follow the expected trends. It is no surprising that the proposed scheme performs better than MRC, though the distance between them is considerably shorter in relation to the Rayleigh channel corresponding figure.

V. Conclusions

In this paper, a new pattern reconfigurable antenna array selection scheme is proposed and analyzed. In particular, assuming the generic scenario where correlation exists between the antenna patterns, a novel analytical framework is developed for describing important statistical characteristics of the proposed scheme. In this context, the PDF, CDF, and MGF of the output SNR are provided and used to analyze its performance using the criteria of OP and BEP. Moreover, simplified expressions are also given for the special cases of independent fading conditions and high SNR values. The new scheme, is applied in a V2V communication scenario, offering essential advantages such as fewer physical antennas as well as fixed hardware complexity in terms of receiving chains. Numerical evaluated results prove that the proposed scheme offers clear diversity gain, with reduced complexity. In our future work we will extend the analysis to the case where non identically distributed fading conditions exist, while the number of states as well as RF chains are more than two.

Appendix
Proof for Theorem 1

In this Appendix the proof of Theorem 1 is provided. The MGF of $\gamma_{\max}$ is given by [17, eq. (20)]

$$\mathcal{M}_{\gamma_{\max}}(s) = \frac{2}{1+s\overline{\gamma}} - \frac{4(1-\rho)}{d_1^2 - 4\rho - s\overline{\gamma}(1-\rho)\sqrt{d_1^2-4\rho}} \tag{A-1}$$

where $d_1 = [s\overline{\gamma}(1-\rho)+2]$. It is noted that substituting (3b) and (A-1) in (2) results to the total MGF of γ_{out}. In order to evaluate the corresponding expression for the PDF the following property of the Laplace transform is used

$$\begin{aligned}\mathcal{L}\left[f_{\gamma_i} * f_{\gamma_{\max}}\right] &= \mathcal{L}\left[\int_0^x f_{\gamma_i}(x-\xi) f_{\gamma_{\max}}(\xi) d\xi\right] \\ &= \mathcal{M}_{\gamma_i}(s)\mathcal{M}_{\gamma_{\max}}(s)\end{aligned} \tag{A-2}$$

where $f_{\gamma_{\max}}(\gamma)$ is the PDF expression of $\gamma_{\max}$ and is given by [17, eq. (18)]

$$\begin{aligned}f_{\gamma_{\max}}(\gamma) &= \frac{2}{\overline{\gamma}} \exp\left(-\frac{\gamma}{\overline{\gamma}}\right) \\ &\times \left[1 - Q_1\left[\sqrt{\frac{2\rho\gamma}{\overline{\gamma}(1-\rho)}}, \sqrt{\frac{2\gamma}{\overline{\gamma}(1-\rho)}}\right]\right].\end{aligned} \tag{A-3}$$

Substituting (3) and (A-3) in the integral provided in (A-2) and after a change of variables, integral of the following form appear

$$\mathcal{I}_1 = \int_0^{\gamma^{1/2}} x Q_1\left[\sqrt{\frac{2\rho}{\overline{\gamma}(1-\rho)}}x, \sqrt{\frac{2}{\overline{\gamma}(1-\rho)}}x\right] dx. \tag{A-4}$$

This integral can be solved in closed form with the aid of [14, eq. (57)] and after some mathematical manipulations and simplifications yields (6) and also completes this proof.

Acknowledgement

This research has received funding from the European Union's Horizon 2020 research and innovation programme under "ROADART" Grant Agreement No 636565.

References

[1] P. J. Smith, A. Firag, P. A. Martin, and R. Murch, "SNR performance analysis of reconfigurable antennas," *IEEE Commun. Lett.*, vol. 16, no. 4, pp. 498–501, Apr. 2012.

[2] D. Piazza, J. Kountouriotis, M. D'Amico, and K. R. Dandekar, "A technique for antenna configuration selection for reconfigurable circular patch arrays," *IEEE Trans. Wireless Commun.*, vol. 8, no. 3, pp. 1456–1467, Mar. 2009.

[3] G. D. Sworo, K. R. Dandekar, and M. Kam, "Analyzing the benefits of pattern diversity for MIMO wireless systems," in *International Conference on Computing, Networking and Communications (ICNC)*, Feb. 2015, pp. 999–1003.

[4] P. N. Vasileiou, K. Maliatsos, E. D. Thomatos, and A. G. Kanatas, "Reconfigurable orthonormal basis patterns using ESPAR antennas," *IEEE Antennas Wireless Propag. Lett.*, vol. 12, pp. 448–451, 2013.

[5] A. M. Alaa, M. H. Ismail, and H. Tawfik, "Spectrum sensing via reconfigurable antennas: fundamental limits and potential gains," *Telecommunication Systems*, vol. 62, no. 3, pp. 581–602, 2016.

[6] M. D. Migliore, D. Pinchera, and F. Schettino, "Improving channel capacity using adaptive MIMO antennas," *IEEE Trans. Antennas Propag.*, vol. 54, no. 12, pp. 3481–3489, Nov. 2006.

[7] S. Poochaya and P. Uthansakul, "Beam tracking in switched-beam antenna system for V2V communication," *International Journal of Antennas and Propagation*, 2016, Article ID 4169619, doi:10.1155/2016/4169619.

[8] M. Shemshaki, T. Zemen, and C. Mecklenbrauker, "Antenna selection diversity for IEEE 802.11p," in *IEEE 39th Annual Conference of the Industrial Electronics Society (IECON)*, 2013, pp. 6876–6879.

[9] A. Chelli, R. Hamdi, and M.-S. Alouini, "Channel modelling and performance analysis of V2I communication systems in blind bend scattering environments," *Progress In Electromagnetics Research B*, vol. 57, pp. 233–251, 2014.

[10] P. Bithas, K. Maliatsos, and A. Kanatas, "V2V communication systems under correlated double-Rayleigh fading channels," in *IEEE Vehicular Technology Conference (VTC)*, May 2016.

[11] H.-C. Yang and M.-S. Alouini, "Markov chains and performance comparison of switched diversity systems," *IEEE Trans. Commun.*, vol. 52, no. 7, pp. 1113–1125, Jul. 2004.

[12] I. S. Gradshteyn and I. M. Ryzhik, *Table of Integrals, Series, and Products*, 6th ed. New York: Academic Press, 2000.

[13] M. K. Simon and M.-S. Alouini, *Digital Communication over Fading Channels*, 2nd ed. New York: Wiley, 2005.

[14] A. H. Nuttall, "Some integrals involving the q-function," DTIC Document, Tech. Rep., 1972.

[15] "IEEE draft standard for information technology - telecommunications and information exchange between systems - local and metropolitan area networks - specific requirements - part 11: Wireless LAN medium access control (MAC) and physical layer (PHY) specifications amendment: Wireless access in vehicular environments," *IEEE Unapproved Draft Std P802.11p/D11.0*, Mar. 2010.

[16] I. Sen and D. W. Matolak, "Vehicle-vehicle channel models for the 5-GHz band," *IEEE Trans. Intell. Transp. Syst.*, vol. 9, no. 2, pp. 235–245, Jun. 2008.

[17] Y. Chen and C. Tellambura, "Distribution functions of selection combiner output in equally correlated Rayleigh, Rician, and Nakagami-m fading channels," *IEEE Trans. Commun.*, vol. 52, no. 11, pp. 1948–1956, Nov. 2004.